NRC Research Press

ARTICLE

Some like it slow: a bioenergetic evaluation of habitat quality for juvenile Chinook salmon in the Lemhi River, Idaho

Richard A. Carmichael, Daniele Tonina, Ernest R. Keeley, Rohan M. Benjankar, and Kevin E. See

Abstract: Management and conservation of freshwater habitat requires fine spatial resolution and watershed-scale and life-stage-specific methods due to complex linkages among land, climate, water uses, and aquatic organism necessities. In this study, we present a valley-scale microhabitat resolution, process-based bioenergetics approach that combines high-resolution topo-bathymetric LiDAR survey with two-dimensional hydrodynamic and bioenergetics modeling. We applied the model to investigate the role of lateral habitat, stream morphological complexity, water use, and temperature regimes on aquatic habitat quality distribution of juvenile Chinook salmon (*Oncorhynchus tshawytscha*) within the Lemhi River (eastern Idaho, USA). Modeling results showed two key aspects: (*i*) a reduction in diverted flows is not sufficient to improve habitat quality potentially because of a legacy of morphological simplification (directly due to straightening and wood removal and indirectly due to low in-channel flows) and (*ii*) morphological complexity and connectivity with side channels and margin areas, which are key and vital elements to support suitable habitats that meet or exceed energetic needs to sustain or promote growth of individuals and populations.

Résumé : La gestion et la conservation des habitats d'eau douce nécessitent des méthodes de haute résolution spatiale, à l'échelle du bassin versant et pouvant cibler des étapes précises du cycle biologique, en raison des liens complexes qui existent entre le paysage, le climat, les utilisations de l'eau et les exigences des organismes aquatiques. Nous présentons une approche bioénergétique basée sur les processus appliquée à l'ensemble d'une vallée et de résolution à l'échelle du microhabitat, qui combine le relevé topobathymétrique par lidar de haute résolution à la modélisation bioénergétique et hydrodynamique en deux dimensions. Nous avons utilisé le modèle pour examiner le rôle des habitats latéraux, de la complexité morphologique du cours d'eau, de l'utilisation de l'eau et des régimes thermiques sur la répartition de la qualité de l'habitat des saumons chinooks (*Oncorhynchus tshawytscha*) juvéniles dans la rivière Lemhi (est de l'Idaho, États-Unis). Les résultats de la modélisation font ressortir deux éléments clés, à savoir (*i*) qu'une réduction des débits détournés ne suffit pas pour améliorer la qualité de l'habitat, possiblement en raison de la simplification morphologique persistante (découlant directement de la rectilinéarisation et du retrait de bois et indirectement des faibles débits en chenal) et (*ii*) que la complexité morphologique et la connectivité avec les chenaux latéraux et les zones marginales sont des éléments clés et d'importance vitale pour soutenir des habitats convenables qui répondent aux besoins énergétiques nécessaires à la croissance d'individus et de populations. [Traduit par la Rédaction]

Introduction

As global human population rise continues, pressure on freshwater resources increases (Davis et al. 2015). An ever-changing climate scenario, coupled with human population growth and its impacts, has begun to put strain on already vulnerable freshwater ecosystems (Woodward et al. 2010). Worldwide concern for conservation of biological diversity and the necessity to limit species loss across the planet has been recognized in both the scientific community (Rand et al. 2012; Isaak et al. 2017) and legislation worldwide (Hering et al. 2010). Native, anadromous fishes, which access fresh water for portions of their life history (Healey 1992), face analogous pressures to global freshwater ecosystems and are in consistent decline, with some populations facing immediate extinction threats (Gustafson et al. 2007). Likewise, local populations, such as those found in the Pacific Northwest of the United States, may rest on tributary restoration and land use changes for recovery (NOAA 2008; NOAA 2011; NMFS 2014). However, our ability to appropriately restore and monitor restoration success and land recovery is uncertain (Bernhardt 2005; Schwartz 2016).

Enhancement of stream habitat has begun to focus on more process-based approaches for restoration to promote and sustain function (Beechie et al. 2010; Wohl et al. 2015). Restorative natural processes may require floodplain reconnection, side channel construction or enhancement, and development of complex habitat provided by wood or other structures to benefit multiple life stages of target species (Bisson et al. 2009; Bennett et al. 2016; Roni et al. 2018; Bond et al. 2019). Improvement of modeling and monitoring techniques is necessary to better characterize ecological uplift in areas in which habitat enhancement has been conducted. The shortcomings of current fish–habitat modeling techniques are widely evaluated and documented, but our ability to understand these links has remained intangible (Schwartz 2016).

Various methods to quantify aquatic habitat quality and quantity have been employed in freshwater ecology and fisheries, including individual-based models (IBM) (Goodwin et al. 2006; Railsback et al. 2013) assessing impacts and interactions of juvenile fish at dams or restorations, microhabitat assessments of salmon nesting patterns (McKean et al. 2008; Benjankar et al. 2016; Kammel et al. 2016), and macroscale, basin-wide analysis (Isaak and Thurow

Received 16 April 2019. Accepted 15 March 2020.

R.A. Carmichael and D. Tonina. Center for Ecohydraulics Research, University of Idaho, 322 E. Front Street, Boise, ID 83702, USA.
E.R. Keeley. Department of Biological Sciences, Idaho State University, Stop 8007, Pocatello, ID 83209, USA.
R.M. Benjankar. Civil Engineering Department, Southern Illinois University Edwardsville, Edwardsville, IL 62025, USA.
K.E. See. Biomark Applied Biological Services, NOAA NWFSC, 2725 Montlake Blvd E, Seattle, WA 98112, USA.
Corresponding author: Richard A. Carmichael (email: rcarmichael@uidaho.edu).

2006) and monitoring of habitat patterns and trends (Cohen et al. 1998; Newson and Newson 2000; Bond et al. 2019). Model inputs have varied with model choice, where multiple univariate inputs such as depth and velocity combined with empirical habitat preference or suitability curves (Maret et al. 2005) have been used to assess aquatic habitat suitability for stream-dwelling fishes (Benjankar et al. 2015). Further, multivariate fuzzy inference approaches attempting to account for interactions of instream habitat characteristics such as depth, velocity, and substrate distribution have also been used for assessing aquatic habitat suitability (Jorde et al. 2001; Noack et al. 2013). With recent advancements in understanding of fish energetic balance, one emergent technique for development of fish–habitat relationships has taken shape as bioenergetic modeling, and in our study specifically we utilize a drift foraging bioenergetics model.

Drift foraging models were originally developed for understanding the mechanics governing habitat selection by salmonids (Rosenfeld et al. 2014), assuming that fish will select habitat that maximizes growth potential. This is achieved by occupying focal points in slow–moderate current, which minimizes energy expenditure, then foraging into adjacent faster currents, which have a higher rate of drift food delivery, thus, maximizing energy gain and growth potential (Fausch 2014). This behavior was first observed in artificial streams in the mid-1950s and early 1960s by fisheries biologists, where larger fish became territorially dominant over areas that maximized their net energy intake (NEI) (Newman 1956; Kalleberg 1958; Chapman 1962; Mason and Chapman 1965). Many bioenergetic models aim to assess the amount of suitable habitat for stream-dwelling fishes through suitability calculations, growth rates, or nutrient availability as indicators of the viability of populations within a given watershed (Chittaro et al. 2014; Keeley et al. 2016; Wall et al. 2016). Thus far, limitations in necessary watershed-scale continuous data have restricted usage of bioenergetics modeling to primarily channel-unit and reach-scale analyses (Guensch et al. 2001; Hayes et al. 2007; Wall et al. 2016). Recent advances in both remote sensing and numerical flow modeling are eliminating some of these constraints. In remote sensing, the advent of topobathymetric LiDARs allows mapping the riverscape at the metre scale, over hundreds of kilometres of stream length, with centimetre accuracy, removing the spatial limitations on continuous coverage of stream geometry (Tonina et al. 2018). Coupling high-resolution bathymetry with two-dimensional numerical modeling of flow hydraulics allows for the derivation of continuous information of flow hydraulics and water quantities over large domains (McKean and Tonina 2013).

Here, we applied these advances to support an energetic mass balance modeling approach (Jenkins and Keeley 2010; Keeley et al. 2016) to assess and understand the impact of water use, water quality, and anthropogenic stream morphological changes (straightening and restoration) on aquatic habitat quality distribution. Our goal is to present a new approach and further the science of bioenergetics modeling with the support of bathymetric LiDAR, built on process-based modeling to investigate aquatic ecosystems broadly across watersheds. We applied this framework to three distinct ~1 km long (60 bank-full channel widths) reaches of the upper Lemhi River (eastern Idaho, USA). The Lemhi watershed is an ideal study area to test such an approach because it supports endangered populations of anadromous fishes, is under strong anthropogenic influences of water use and habitat alteration, and has readily and publicly available spatially continuous or spatially explicit data, including LiDAR-supported bathymetry, discharge measurements, macroinvertebrate drift density, stream temperature, and juvenile fish size.

Methods

Study site

The Lemhi River is a tributary of the Salmon River, ~100 km long between its origin near the town of Leadore (Idaho, USA) and its confluence with the Salmon River, near the town of Salmon (Idaho, USA). Its drainage area encompasses 3300 km² of forest, range, and irrigated farmland. The basin supports wild populations of threatened Chinook salmon (*Oncorhynchus tshawytscha*) and steelhead trout (*Oncorhynchus mykiss*), listed under the US Endangered Species Act (NMFS 2014). Chinook salmon of the Columbia River basin (where the waters of the Lemhi eventually flow) provide major socioeconomical benefit, including food production such as commercial fishing, recreational fishing, subsistence fishing, and nutrient cycling services, and are of important social and cultural value (Morton et al. 2017). The Lemhi River supports a full range of freshwater Chinook salmon life stages, beginning with a return of spawning adults in the spring (spawning in the late summer – early fall), juvenile emergence in March, over-winter rearing of juvenile Chinook salmon parr and presmolts, to an outmigration of age-1 smolts in the spring (Bjornn 1971). Yet, large water withdrawal for irrigation during the agricultural growing season, between May and October, have drastic impacts on stream habitat and the ecosystem of the Lemhi basin, shifting flow timing, lowering critical summer flow, and potentially reducing habitat quality for key life stages (Walters et al. 2013). Anthropogenic activities have also changed the stream alignment, via straightening and loss of floodplain connectivity by removing and limiting lateral channels.

Study reaches

We chose three reaches in the upper Lemhi River, each ~1 km long, to model the bioenergetic profitability for juvenile Chinook salmon (Fig. 1). The three study reaches were selected to represent a broad range of morphologies typically encountered in a meadow system, with a mix of straight, meandering, and multithread systems, including an engineered restored reach. These reaches are also in close proximity to one another such that they have similar discharge, stream water temperature, and macroinvertebrate drift rates.

The most upstream reach, referenced as the Straight reach, is a single thread, straight, nearly trapezoidal, simplified channel, confined in parts by a highway that parallels this section. The middle reach, referred to as the Complex reach, is a multithreaded channel with side branches and meanders within a meadow setting. The reach has variable amounts of streamside vegetation and instream habitat conditions. The most downstream reach is an engineered, restored channel that was completely redesigned as a stream enhancement project. The engineered channel is a new reach dug into the floodplain, and the prerestoration straight channel was abandoned and closed off. For this restored section, we modeled two scenarios: (*i*) a two-thread system with the prerestoration, straight channel functioning as a side channel, called the Restoration Open reach, where the two channels are open and functioning in parallel and (*ii*) a single thread system without a side channel, called the Restoration Closed reach. In the former case, flow splits between the two reaches depending on the local geometry of the system. The natural diversion of the flow between the two channels allowed us to quantitatively compare results between these two restoration scenarios.

Each study reach experiences large amounts of upstream dewatering via diversions for agricultural production. We chose to model two temporal periods, which differ by flows (diverted and undiverted) and water temperature for each reach of interest and resulted in a total of four scenarios through four distinct reaches.

Fig. 1. Map of the Lemhi watershed and spatial locations of each study site: Complex, Restoration, and Straight. The inset shows the location of the Lemhi drainage within the state of Idaho, USA. The map is displayed over imagery from the National Agriculture Imagery Program; coordinates are in GCS North American 1983. [Colour online.]

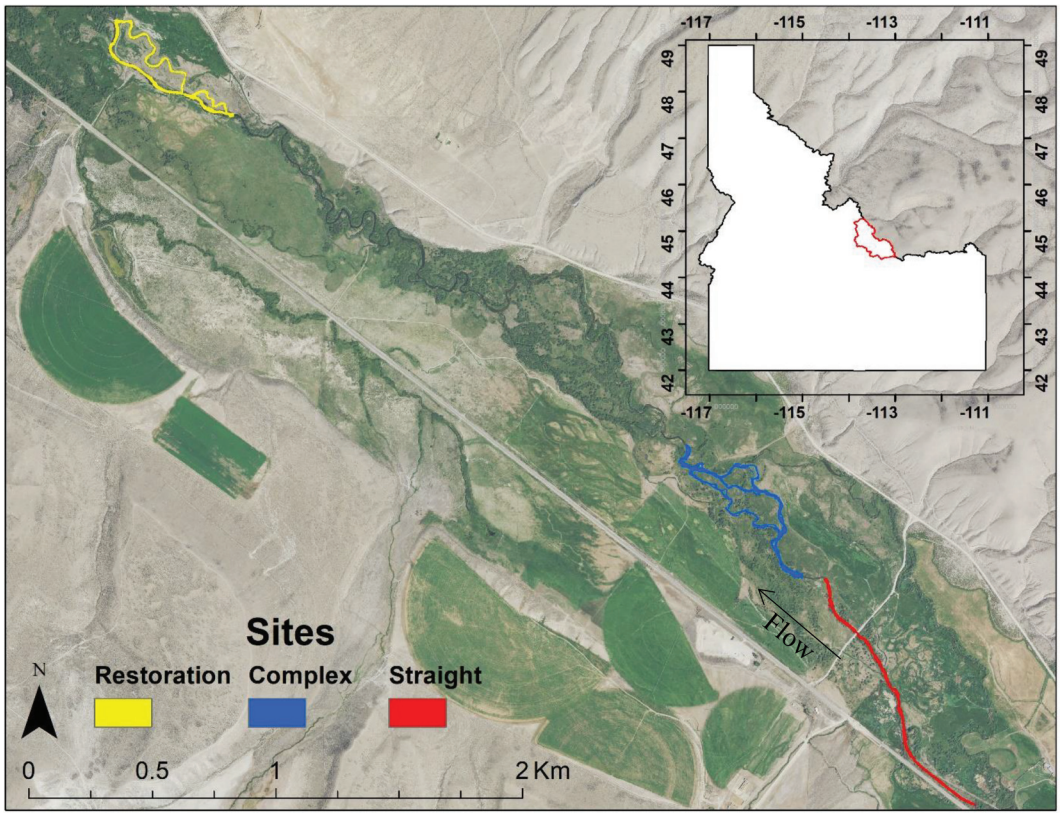

Modeled scenarios

To assess the effects of water use for all reaches, we modeled both a diverted and an undiverted flow condition for two critical periods: late summer (August) and fall (October) (Fig. 2). A late August period was selected because all water diversions are typically in use, discharge is near the lowest amount of the year, and water stream temperatures are high (weekly mean ~ 12 °C). Conversely, the last part of October has all diversions closed, hydrology follows a natural flow regime, and stream water temperatures are still warm and relatively mild (weekly mean ~ 7 °C) with fish feeding and rearing. Late October has been suggested to be a critical period, as many young, rearing fish leave the Lemhi as presmolts to move to the Salmon River (Copeland et al. 2014), indicating that habitat may not be suitable for presmolt fish.

To test the impacts of water management and flow hydraulics on our study reaches (e.g., depth and velocity), we held all input parameters constant except for discharge for two alternative flow scenarios: (*i*) for a more natural flow regime during August, we chose the same discharge volume as October, and (*ii*) to test an alternative water management scenario for October, we modeled a reduced discharge equal to that of August. These alternative scenarios allowed us to estimate the change in suitable area as a function of water management alone.

Modeling

The modeling can be explained as a two-step approach. First, we developed and validated a two-dimensional numerical flow model supported by high-resolution bathymetry to model depth and velocity at a 1 m resolution across each study reach. Second, we used depth and velocity and combined them with available biological information, including temperature, aquatic invertebrate drift density, and juvenile Chinook salmon size distributions to populate a spatially explicit bioenergetics model across all of our modeling scenarios and reaches.

Hydraulic modeling

High-resolution topobathymetric surface

Bathymetric LiDAR data were collected in the fall of 2013 with the Experimental Advanced Airborne Research LiDAR-B sensor for the entire mainstem Lemhi River (Tonina et al. 2018). From the original point cloud, a 1 m digital elevation model (DEM) was derived for both stream and floodplain topographies. The DEM was extensively validated by comparing LiDAR survey with a high-resolution, high-accuracy differential global positioning system (D-GPS) real-time kinematic survey instruments at three test beds with high resolution (1.6 points·m^{-2}). The comparison showed root mean square error (RMSE) and median absolute error of 0.11 m for the submerged topography (Tonina et al. 2018). The dataset was further validated at 454 centerline points spaced evenly along the upper 25 km of the dataset, with RMSE and median absolute error slightly higher at 0.13 m. The test-bed ground survey was conducted only a few months apart from the LiDAR survey without any high flows between surveys; the measurements at the valley scale along the centerline were collected 3 years after the LiDAR survey. Thus, some topographical changes may have occurred between the LiDAR and the valley-scale ground measurements, but changes are unlikely between the LiDAR and test-bed ground survey.

Numerical flow model

A calibrated and validated two-dimensional hydraulic model (Danish Hydraulics Institute Mike 21; Danish Hydraulic Institute 2000) supported by a 1 m resolution DEM derived from the bathy-

Fig. 2. Maps of the Lemhi River stream channel wetted area of each study site according to different restoration and modeling scenarios during August (fully diverted, warm stream temperatures) and October (undiverted, cold water temperatures): (A) fully diverted Complex; (B) fully undiverted Complex; (C) fully diverted Straight; (D) undiverted Straight; (E) fully diverted Restoration Closed; (F) undiverted Restoration Closed; (G) fully diverted Restoration Open; (H) undiverted Restoration Open. [Colour online.]

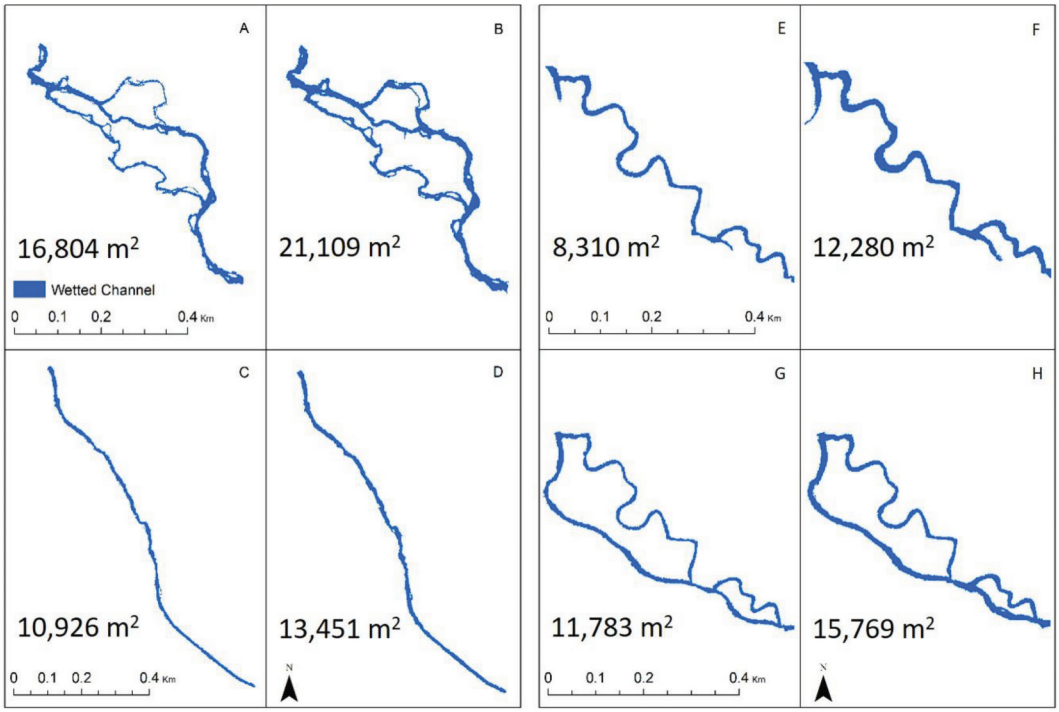

metric LiDAR survey, serving as the defined boundary condition, quantified stream water depths, and depth-averaged velocities for the modeled discharges. The numerical model solves the two-dimensional Reynolds averaged Navier–Stokes equations with the Boussinesq turbulence closure (Danish Hydraulic Institute 2000). It has two coefficients that need to be assigned: lateral eddy viscosity constant and Manning's n. Both coefficients were set as spatially constant, the former with a constant value of 0.15 $m^2 \cdot s^{-1}$ and the latter of 0.025 $s \cdot m^{-1/3}$ for the entire system. The Manning's n value was selected by minimizing the RMSE between measured and predicted depth-averaged velocity and water surface elevation. Its value was close to that quantified with the Strickler's equation $n = 0.026\ s \cdot m^{-1/3} = D_{50}^{1/6}/21.1$, based on the median diameter of the stream bed material, D_{50}, which was 0.03 m for these reaches of the Lemhi River. The RMSE for velocity was 0.19 $m \cdot s^{-1}$ and for water surface elevation was 0.03 m at low summer discharges (~2 $m^3 \cdot s^{-1}$) at the test-bed locations where the DEM was analyzed.

The selected Manning's n was then validated by comparing measured water surface elevation to modeled water surface elevation and measured depth-averaged flow velocity to modeled depth-averaged flow velocity. These data were collected at different discharges during late October (still low to guarantee safety during measurements but higher, approximately double, from those of the calibration) and locations along the upper 32 km of the Lemhi River where the three study sites were located. Validation of the model resulted in RMSEs of 0.11 m, 0.18 m, and 0.2 $m \cdot s^{-1}$, for water surface elevation, depth, and velocity, respectively. The larger errors with respect to the test beds could be due to two sources: topographic changes and less constrained discharge. This second set of ground data was collected 3 years later than the LiDAR survey, which supports the hydraulic modeling. During this time, some bathymetric changes may have naturally occurred, which could explain the higher errors between predicted and measured bathymetry and water depths. Additionally, discharge was well characterized in the test beds, but constraining it at larger scales than the test beds was very challenging due to the large number of diversion dams, which may be fully or partially withdrawing water. Thus, some of the error in predicting the depth and velocity may be a result of a less constrained discharge imposed on the hydraulic model that may have been different from the real one. However, these calibration and validation results were near published acceptable values for numerical flow modeling (e.g., Kammel et al. 2016).

Flow scenarios

The two-dimensional model was run for a set of representative discharges, which spanned the daily mean hydrograph recorded for the Lemhi River at Cottom Lane, Idaho Department of Water Resources (IDWR) gauging station, located just downstream of the study reaches. From this set of discharges, we selected those closer to the mean weekly discharges of the last weeks of August (2 $m^3 \cdot s^{-1}$) and October (5 $m^3 \cdot s^{-1}$; Fig. 3).

Bioenergetics–foraging model

Feeding locations

Feeding locations for juvenile Chinook salmon were simulated using a geographic information system (GIS) software (ESRI ArcGIS 10.6). We interrogated cross-sections in the model grid perpendicular to the centerline of all wetted channels (including main and off-channel areas consisting of side channels and backwaters) for each reach at 3 m intervals to reduce overlap in sharp meander bends. We then interrogated points every 1 m along each individual cross-section. We chose to interrogate points every 1 m to match the 1 m by 1 m resolution of the modeled depth and velocity output rasters. We then performed an Extract Value to Point (ESRI, 2017) with the feeding locations and modeled output rasters to extract depth and velocity values at each individual point.

Fig. 3. Daily average discharge (solid black line) and its 75th (upper black dotted line) and 25th (lower black dotted line) percentiles calculated from all available discharge measurements at the Lemhi River at Cottom Lane Idaho Department of Water Resources gauging station just upstream of the study sites where we modeled August at 2 $m^3 \cdot s^{-1}$ and October at 5 $m^3 \cdot s^{-1}$. The solid blue line indicates the daily average temperature corresponding to the value on the right vertical axis where the temperatures chosen to populate the model were August at 11.93 °C and October at 6.97 °C. The solid black rectangles represent the modeled temporal periods of the last week of August and last week of October. [Colour online.]

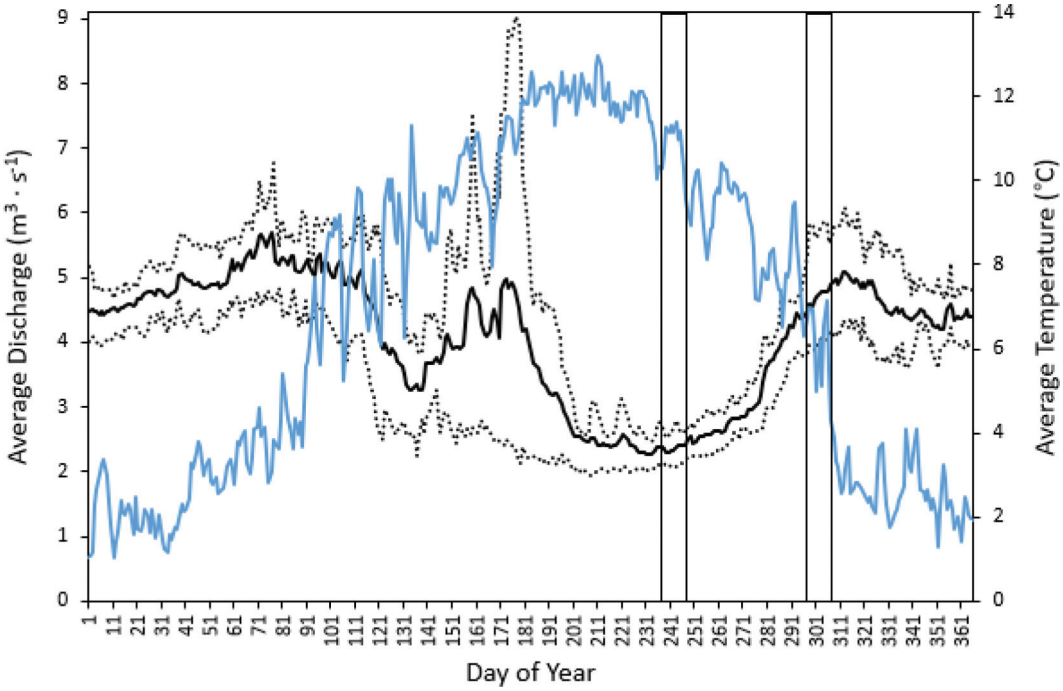

Bioenergetics model

We used a bioenergetic drift-foraging model to calculate the rate of net energy intake (NEI ($J \cdot h^{-1}$) i.e., energetic profitability) of each feeding station or point location on interrogated cross-sections. The foraging model was originally developed by Hughes and Dill (1990), further developed and tested by Guensch et al. (2001) and Jenkins and Keeley (2010), and later applied by Keeley et al. (2016). The model input variables consist of water depth and depth-averaged velocity, juvenile Chinook salmon fork length and estimated mass, drift density binned by size class, and stream water temperature. The model assesses the amount of energy per hour available in the stream as captured food, minus the cost of capture, swimming, metabolism, and excretion following the relationships described in Jenkins and Keeley (2010) and Keeley et al. (2016). We leveraged Elliott (1975) for estimating maximum food ration (C_{max}) that could be ingested by a salmonid of a given size over an 8 h period of active foraging, such that NEI = $C_{max} \times E_i$ – SC, if GEI ≥ C_{max}; otherwise, NEI is estimated with the following equation:

$$\mathrm{NEI} = \frac{\sum_{i=1}^{4} \mathrm{MCA}_i \times V_{avg} \times \mathrm{DD}_i \times \mathrm{PC}_i \times (E_i - \mathrm{CC}_i) - \mathrm{SC}}{1 + \sum_{i=1}^{4} t_i \times \mathrm{MCA}_i \times V_{avg} \times \mathrm{DD}_i}$$

We calculated the maximum capture area for each prey size class i (MCA_i), mean water column averaged velocity at each feeding station (V_{avg}), drift density for each prey size class (DD_i), the probability of capturing prey (PC_i), energy acquired from each food item captured (E_i), the cost associated with capturing the prey item (CC_i), swimming costs associated with holding a foraging position at each feeding location (SC), and the time spent handling the prey item (t_i). In our study, we used four size classes of prey. Further information on model details, calculations, and equation sources can be found in Keeley et al. (2016) (also refer to their supplementary table 2).

NEI accounts for all energy intake per hour through feeding minus the energy expended for gathering and consuming the food, such that a NEI = 0 means that all energy extracted from the food ingested has been consumed and no energy is available for growth. To assess the amount of surplus energy available for growth, we compared daily NEI (DNEI (J)) with a maximum growth ration (MR) by dividing DNEI by MR. We assumed an 8 h foraging duration to represent the amount of time a fish may forage each day, such that DNEI = NEI × 8 h. To estimate the amount of required energy to support a maximum growth ration, we used the empirically derived equations developed by Elliott (1976) and modified by Jenkins and Keeley (2010) to provide MR (J):

$$\mathrm{MR} = 0.58a \times \begin{cases} 1.39 M_{\mathrm{Fish}}^{0.716} e^{0.224 \times T} & \text{if } T \le 6.6 \\ 2.711 M_{\mathrm{Fish}}^{0.737} e^{0.105 \times T} & \text{if } T > 6.6 \end{cases}$$

where M_{Fish} (mg) is the fish mass, T is the stream water temperature (°C), a = 18.5810 ($J \cdot mg^{-1}$) is a constant, which converts mass to Joules, and 0.58 is the energy assimilation as suggested by Gustafson et al. (2007) and Elliott (1976).

Comparison between DNEI and MR quantifies whether the fish captured enough food to promote growth at different levels. We introduced the ratio (AE) between DNEI and MR as an index of available energy for growth. A value of AE = 1 means that the location provides enough energy for maximum growth potential, and values less than 1 indicate reduced growth potential. For instance, values larger than 1 provide more energy than needed by a single fish for maximum growth potential. We quantified AE at each feeding station for the modeled temperature of each scenario and 50th percentile of observed fork lengths and used this value to assess suitability throughout the entirety of the study areas. If the

calculated ratio was equal to or greater than 1, the location was labeled as suitable; conversely if the resulting value was less than 1, the feeding station was classified as unsuitable.

Temperature

Water temperature along the Lemhi River was collected with in-stream deployed Onset Hobo Tidbits by the Columbia Habitat Monitoring Program (CHaMP 2014). The nearest monitoring site was ~1 km downstream of the study sites. We quantified the weekly average temperature of the last week of August 2016 and October 2016 from hourly temperature observations as input data into the bioenergetic model. Each reach and scenario were modeled with spatially uniform temperatures for both the August and October scenarios.

Juvenile Chinook salmon length and mass

We obtained all length and mass information of juvenile Chinook salmon from the publicly available dataset developed as part of the Integrated Status Effectiveness Monitoring Program (ISEMP). The dataset contains information collected from both summertime electrofishing mark–recapture studies and rotary screw operations in the Lemhi River watershed. The fish sampling targets juvenile Chinook parr and presmolts prior to overwintering and migration in the spring as 1-year-old smolts. We calculated the 25th, 50th, 75th, and 90th percentiles of fork length (FL) for juvenile Chinook salmon from the available fish data to identify the range of fish sizes to be modeled in the bioenergetic evaluation of habitat quality for each study reach. We used a linear regression model ($M_{\text{Fish}} = 3.18 \times F_l - 5.24$, $R^2 = 0.96$) to quantify the relationship between fork length and fish mass to calculate the mass of each *i*th percentile of observed fork lengths, where F_l is equal to the measured fork length of interest, and M_{Fish} is the mass of the given fish at a given fork length.

Drift density

To estimate food availability for juvenile salmon, we used counts and lengths of captured, drifting macroinvertebrates obtained from the habitat evaluation program CHaMP (CHaMP 2014). The captured drifting invertebrates were binned into four equal length size class bins of 3 mm, with the smallest size class of less than 3 mm and the largest between 9 and 12 mm (Table 1). The total volume of water that passed through each net was used to create a drift density of invertebrates, where the total number of invertebrates captured in each size class was divided by the total volume of water sampled (DD_i). Our observed values of drift were within the range of what others have reported in the literature (Allan 1978; Wilzbach and Hall 1985; Leung et al. 2009; Jenkins and Keeley 2010).

Typically, two nets were deployed (1000 μm mesh, 40 cm × 20 cm mouth openings) side by side in the thalweg, where freely drifting invertebrates within the water column and on the surface were captured in the net and collected in a cup fixed to the back of the net. Precautions during net deployment were taken to ensure that benthic invertebrates did not crawl into the net by raising net bottoms roughly 2 cm above the streambed. Additionally, deployment times occurred during optimal daytime conditions, avoiding crepuscular periods (Weber et al. 2014; Wheaton et al. 2018). The volume of water sampled by each net was calculated using a measured depth averaged velocity (measured at 60% of the net depth), water depth sampled by the net, and the width of the net before and after net deployment. Those three measurements were then multiplied by the duration of the sample to obtain a total volume of water sampled for each drift net (m^3). Because of funding limitations and limited available drift data, we assumed a constant drift rate for all modeled reaches and scenarios. Further information on methods used for capturing drifting macroinvertebrates can be found in the CHaMP protocol (CHaMP 2014). We used the available CHaMP data from the sampling site most closely located to our three reaches to generate drift rates needed to populate the bioenergetics model.

Table 1. Prey size class bins and corresponding drift density (DD_i) values used to populate the model.

Prey size (mm)	Drift density (no. of prey·cm^{-3})
0–3	2.004
3–6	0.9420
6–9	0.0856
9–12	0.0054

Analysis

The first step in analyzing the bioenergetic results was to calculate the percentage of modeled feeding stations that either met or exceeded the maintenance ration, AE ≥ 1, to generate the percentage of each reach or scenario suitable for juvenile Chinook salmon at all modeled fork lengths (Fig. 5). Further analysis was confined to modeling the 50th size percentile (75 mm fish) because there was little variation in the percentage of suitable feeding locations with fish size, and model processing times were lengthy.

We analyzed AE both as statistical values via frequency distribution, which allowed comparison among sites, and as spatial information as maps. The latter allowed us to analyze the spatial distribution of AE and visualize correlation between hydromorphological variables and AE values. We separated the analysis into the main channel and side channels to gain an understanding of the contributing total area of suitable habitat by the off-channel areas. We calculated the wetted areas of main and off-channel areas and then multiplied these values by the fraction of feeding locations that met or exceeded the maintenance ration, AE ≥ 1. This result provided us with an estimate of suitable area for the main and off-channel habitat. Lastly, we estimated the percentage of suitable feeding habitat in each reach or scenario contributed by the off-channel.

Results

In the August scenario, AE equaled or exceeded 1 over more than 95% of the total area in all reaches regardless of main and off-channel location or presence of off-channel habitat. Suitability expressed as percentage of area that met or exceeded a maximum growth ration, with AE ≥ 1 slightly increased with fork length for the August fully diverted scenario in all reaches (Fig. 4). Conversely, during the undiverted, late October scenario, the percentage of suitable habitat decreased sharply for all fish sizes compared with the results from the August modeled scenario. In October, the percentage of suitable habitat also decreased with increasing fish size in all reaches. The sharp decrease in areas with AE ≥ 1 from August to October is most notable in the main channel of each study site (Fig. 5). During late October, the only remaining suitable habitat was near the margins of the main channel and off-channel areas, which are composed of side channel and backwater habitat. The Complex and Restoration Open reaches had the greatest amount of high-quality habitat (largest percentages of AE > 1 (and AE > 3)) for both scenarios modeled, August and October (Fig. 6).

These two reaches had the highest percentage and amount (m^2) of suitable off-channel habitat for 75 mm Chinook salmon in both August and October flow scenarios (Figs. 7 and 8). All three modeled reaches that contained off-channel habitat exhibited a decline in the area and percentage of suitable habitat from the August to the October flow scenarios (Fig. 7). The Complex and Restoration Open reaches had the greatest amount of off-channel suitable habitat, followed by the Restoration Closed reach. Off-channel habitat did not contribute to the total area of suitable habitat in the Straight reach, because it had none. The Restoration Open reach had the second largest area of suitable habitat, including in the off-

Fig. 4. Calculated fraction of suitable habitat, defined as AE ≥ 1, modeled daily net energy intake (DNEI) values meeting or exceeding the required maintenance ration for a given fork length, drift abundance, and temperature. Results are grouped by reach or flow scenario and shaded by modeled fork lengths of 65 mm (black), 75 mm (gray), 88 mm (hatched), and 102 mm (open), from left to right.

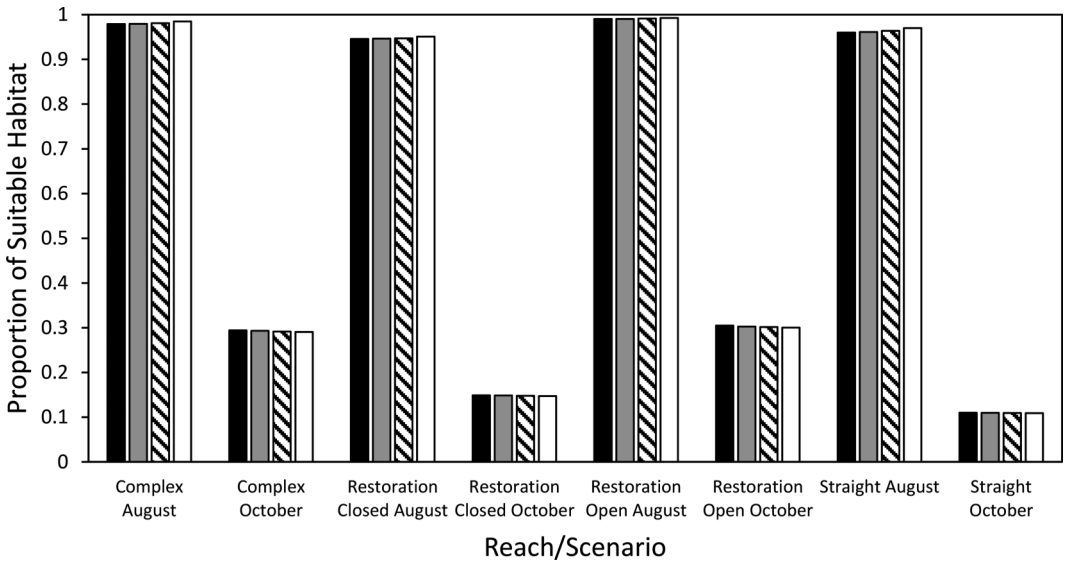

Fig. 5. Spatially distributed results of all modeled feeding locations that either met or exceeded the calculated maintenance ration (AE ≥ 1) for each reach and scenario (August, October) and the 50th percentile (75 mm) fork length of measured Lemhi River Chinook salmon. [Colour online.]

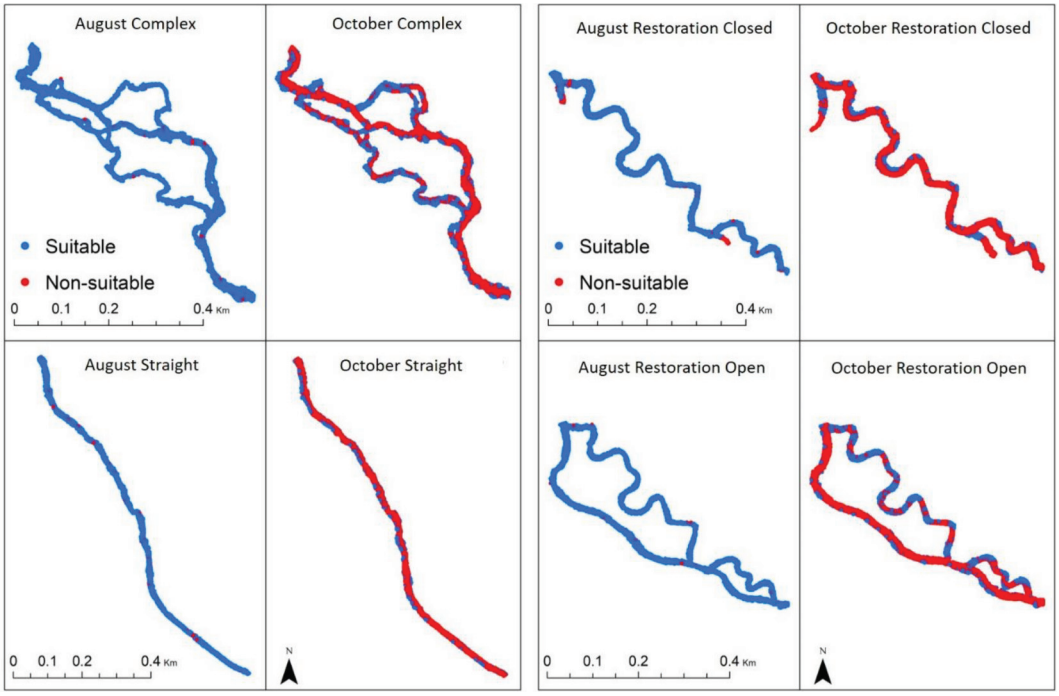

channel, followed by the Restoration Closed scenario, and lastly the Straight reach. The percentage of off-channel suitable habitat contributing to the total area of suitable habitat in the modeled reaches with side channels increased from the August to October flow scenarios (Fig. 8). Both the Complex and Restoration Open reaches had the largest percentages of suitable off-channel habitat, with the largest percentage occurring in the Restoration Open reach for both flow scenarios. The undiverted, late summer alternative flow scenario (increased discharge) decreased the area and percentage of suitable habitat in all reaches (Fig. 9). The Straight reach exhibited the greatest percentage reduction, followed by the Restoration Closed reach and the Restoration Open reach. Similarly, the late October undiverted flow scenario supported less suitable habitat area than the decreased, diverted discharge scenario (Fig. 10).

Discussion

Similar to other studies, our results show that floodplain reconnection and side channel construction–reconnection may be necessary to restore natural, sustainable processes and improve channel function and habitat complexity (Bisson et al. 2009; Roni et al.

Fig. 6. AE, defined as the ratio of DNEI to maintenance ration, for both (A) August (diverted) and (B) October (undiverted) modeled scenarios. The *y* axis displays the proportion of habitat area that falls within each bin of AE (*x* axis). The bars are shaded by the corresponding reach for the 50th percentile fork length. The dotted line marks a bin value of 1 or greater, which indicates feeding stations have met or exceeded the calculated maintenance ration.

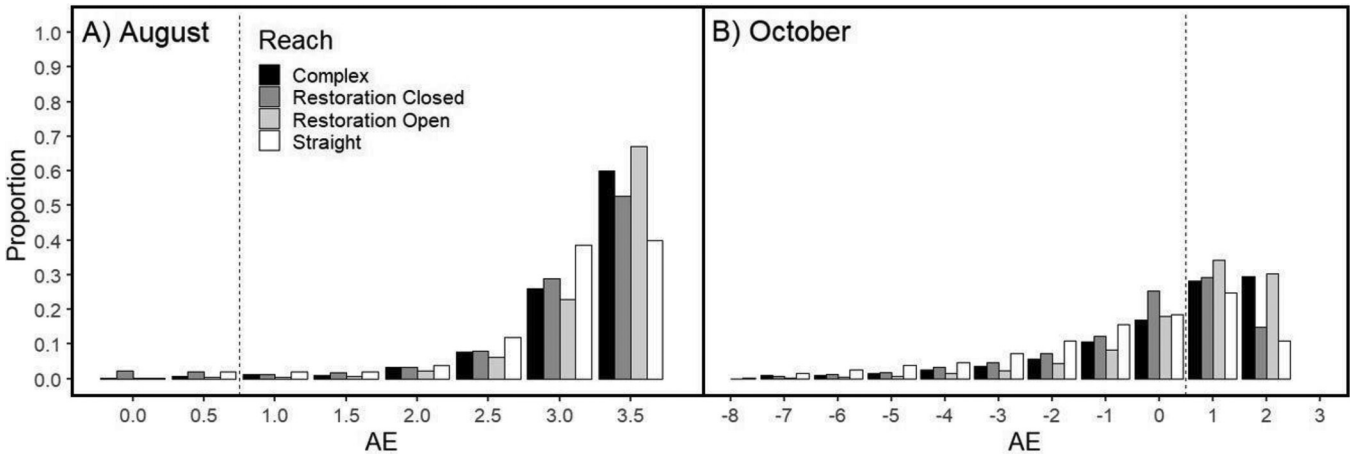

Fig. 7. Total amount of suitable habitat (AE ≥ 1) for the entire reach (black bars), its main channel (hatched bars), and off-channel areas (open bars) for the 50th percentile of fork length (cm) for Lemhi River juvenile Chinook salmon.

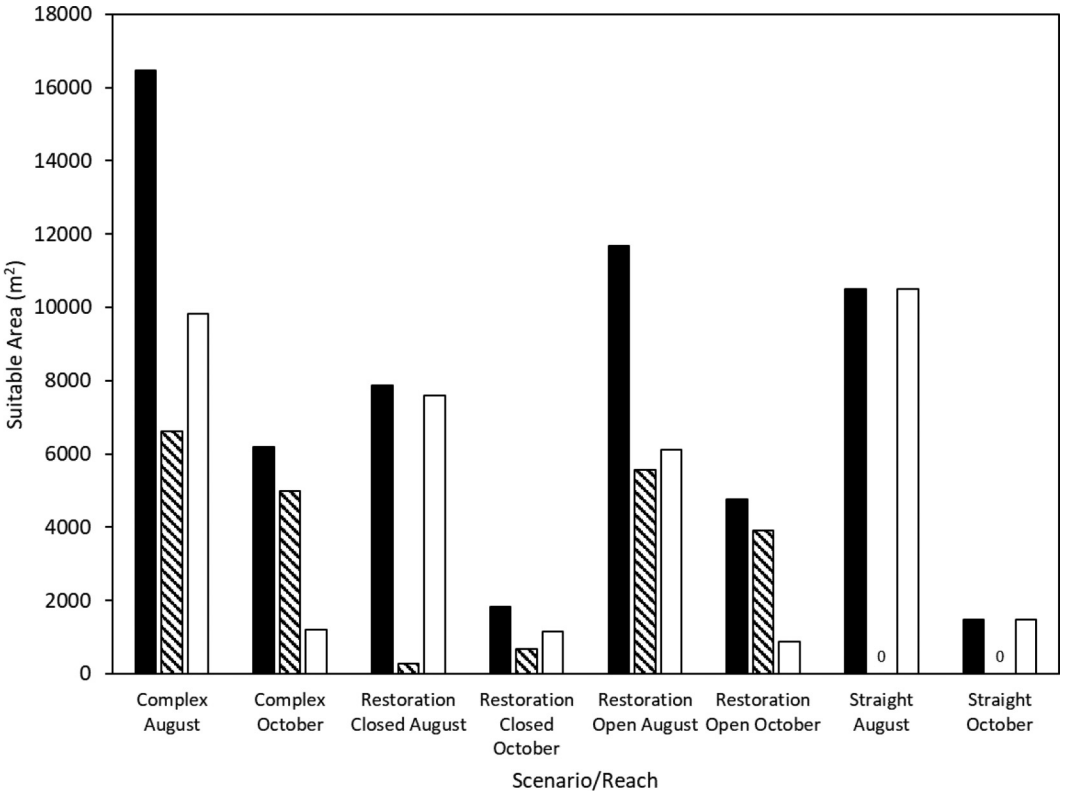

2018). The Columbia River basin has experienced a loss of floodplain habitat, and our results help support the assumption that in general, watersheds throughout the western United States would benefit from floodplain enhancements (Bond et al. 2019). Further, restoring channel function through side channel construction or reconnection will help mitigate habitat loss for juvenile Chinook salmon (Figs. 5 and 8). Our study and similar analyses may also provide insight into the cost–benefit of channel enhancement through pre- and postrestoration modeling (Fig. 7).

The undiverted summer scenarios predict that as water is returned to the channel through tributary reconnections, minimum flow requirements, and reduction in irrigation diversion flows, an already simplified channel may not have the morphology to substantially improve suitable habitat for juvenile salmonids. Simplified morphology includes small variation in depth and velocity, associated with shallow pools and low amplitude riffles, lack of lateral channel (off-channel) and margin habitats — or connectivity between these and the main channel. Reaches with complex features such as margin habitat and side channels maintain suitable habitat at high flow and, in our case, buffer the decline in overall habitat suitability from August to October. As diverted flows are decreased, a simultaneous effort should focus on restoring channel processes, including reconnection and engineering of secondary and backwater channels (Wohl et al. 2015).

Fig. 8. Percentage of off-channel habitat estimated as suitable (A) and percentage of off-channel contribution to the total suitable area (AE ≥ 1) of each individual study reach (B), where the black bars represent August and the open bars represent October.

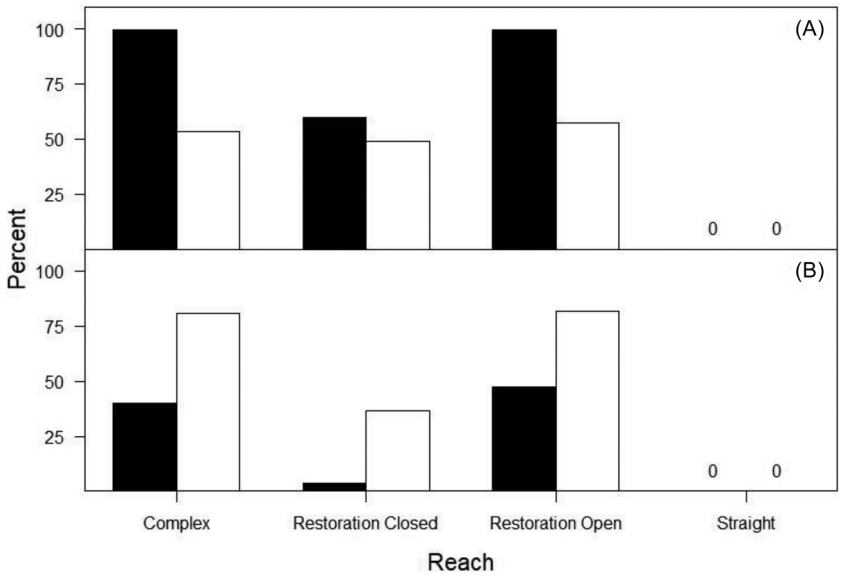

Fig. 9. Total percent suitable (AE ≥ 1) habitat (A) and total suitable area (B) for the late August alternative flow scenario, assessing the impacts of hydraulics by increasing discharge (all other variables held constant) modeled at the diverted August discharge (black bars) and the undiverted October discharge (open bars).

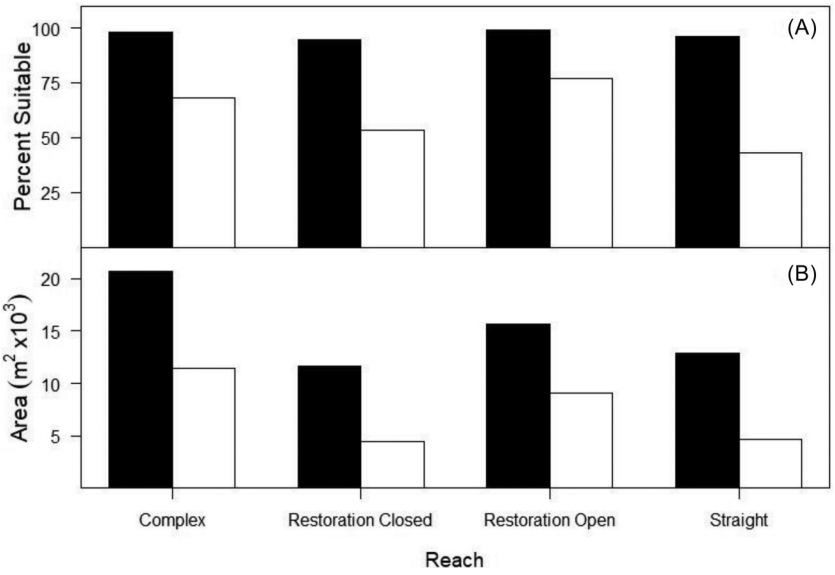

A previous study of fish bioenergetics showed that cutthroat trout (*Oncorhynchus clarkii*) preferred slower, deeper pool habitat (Jenkins and Keeley 2010). Further, 1-year-old salmonids showed greater growth potential in deeper, slower water, potentially seeking out habitat that promotes growth, including pools (Rosenfeld and Taylor 2009; Rosenfeld and Boss 2011). Our results support this finding, where areas of slower water and lower flows have a higher calculated NEI and a greater amount of suitable habitat for juvenile Chinook salmon. These suitable habitats are observed when the engineered and the original main channel can function as a two-thread system rather than diverting flow solely into the engineered channel (Fig. 4 and 5). Further, our alternate water management scenario demonstrates that when return flows are moderated, this results in a greater estimated area of suitable habitat (Fig. 10). Increasing channel flow should be accompanied by a restoration of channel form (Palmer et al. 2010), and restoration projects must consider multiple flow scenarios and life stages of target species to better address limiting factors within watersheds (Schwartz 2016) (Fig. 9).

Several studies within the Lemhi River basin have shown that streamflow is a good predictor of juvenile survival to the ocean (Arthaud et al. 2010; Walters et al. 2013). In a climate change scenario, modeled to 2040, Arthaud et al. (2010) estimated that undiverted streamflow is projected to increase juvenile survival by 42%–58%. In addition, tributary flow during early rearing is a good predictor of survival and productivity, but mainstem Columbia River flow was the best predictor (Walters et al. 2013). Conversely, our study shows that high flows may decrease the amount of available habitat or capacity for juvenile fish. From August (fully diverted) to October (fully undiverted) discharge, the overall bioenergetic suitability of our study reaches declined drastically, mainly due to increase in water velocities rather than change in

Fig. 10. Total percent suitable habitat (A) and total suitable area (B) for October, modeled at the diverted discharge (black bars) and the undiverted discharge (open bars).

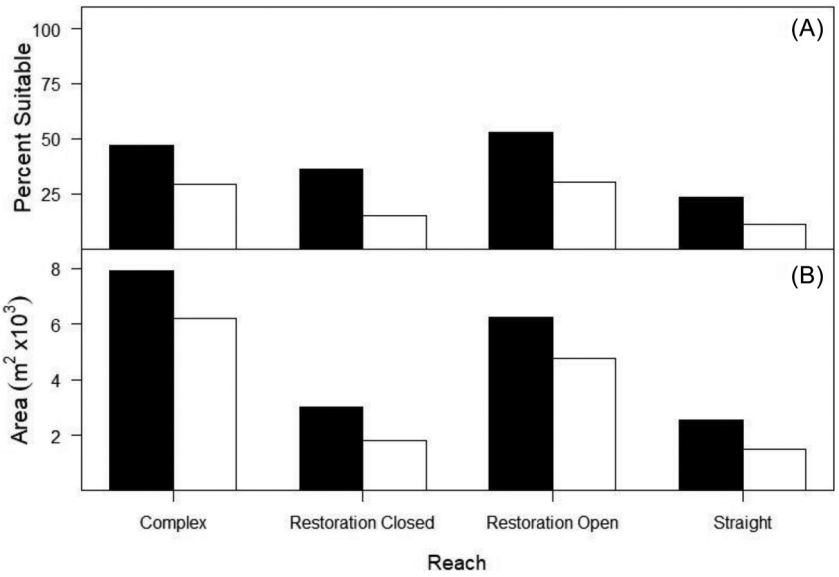

water temperatures (Figs. 4, 5, and 6). Walters et al. (2013) assessed change in habitat suitability by correlating the change in channel unit area and flow from diversion removal with overall survival and productivity. It is possible that our study may not properly characterize all the mechanistic interactions between juvenile fish and their rearing habitat, most likely due to the assumption of uniform nondepletion of drift throughout our reaches. However, our model does incorporate not only spatially distributed depths and velocities, but also temperature and food availability in quantifying the habitat quality for juvenile Chinook salmon, so our results may further help explain why mainstem flow is a better predictor of survival rather than tributary flows. Our result parallels what Jenkins and Keeley (2010) reported; fish in the Salmon River basin can maintain high growth rates during the summer months, but habitat suitability might decline in October. The reduction in suitable habitat may explain the outmigration of many juvenile Chinook salmon in the Lemhi basin in the fall as presmolts (Bjornn 1971; Copeland et al. 2014) rather than the following spring as true 1-year-old smolts. This is another line of evidence supporting why juvenile to adult return rates are better predicted by mainstem river flow rather than tributary flow (Arthaud et al. 2010).

Limitations in this type of modeling have been documented, and improvements to modeling have been suggested (Hayes et al. 2007; Jenkins and Keeley 2010; Wall et al. 2016; Dodrill et al. 2016; Naman et al. 2017). Wall et al. (2016) overpredicted salmonid carrying capacity of their study sites when model estimates were validated against measured fish densities, and they attributed this to an assumption of constant drift densities throughout their study sites. In our study, potential overestimations of habitat quality could be due to the utilization of a non-Chinook salmon specific maintenance ration. However, habitat quality could be underestimated using a maximum growth ration as opposed to a reduced maintenance or growth ration for calculation of AE. The maintenance ration equation used in this study was originally developed for brown trout (*Salmo trutta*) and may not characterize the energetic needs of Chinook salmon properly. Although, other studies have used this technique (e.g., Jenkins and Keeley 2010; Keeley et al. 2016), incorporation of a Chinook-specific maintenance ration may be necessary (Deslauriers et al. 2017). Parallel to Wall et al. (2016), we assumed that drift (density) was spatially evenly distributed throughout all reaches, and it is likely that this is not the case. We did not account for drift depletion due to foraging from other species or competition among the same modeled species. Yet, our measured drift densities were well within limits reported by other studies of one to five invertebrates per cubic metre to as many as 20 to 50 invertebrates per cubic metre (Allan 1978; Wilzbach and Hall 1985; Leung et al. 2009; Jenkins and Keeley 2010). A more appropriate but time-consuming method may be to model reaches and scenarios across a range of drift densities observed in the literature for streams like the Lemhi. Additional limitations may include inherent error in the numerical modeling process and outputs, but studies have shown that the accuracy of bathymetric LiDAR is sufficient to support two-dimensional hydrodynamic modeling with acceptable levels of error in the resulting modeled depths and velocities (McKean et al. 2014; Tonina et al. 2018). Such errors associated with numerical modeling supported by topobathymetric LiDAR may be greater than traditional measured depth and velocity or numerical modeling supported by total station survey (the accuracy of which is less than 1 cm), dGPS (accuracy ~3 cm), or cross-sectional analysis (Keeley et al. 2016; Wall et al. 2016). However, traditional ground survey techniques (e.g., dGPS, total station) are generally limited in extent to a few channel widths in long reaches (Legleiter et al. 2011; Brooker 2016; Kammel et al. 2016). These surveys may have high local topographical accuracy but low resolution (less than one point per square metre) to capture large-scale topographical features. Thus, the ability to model much greater distance and areas encompassing all lateral habitats may outweigh the shortcomings of increased local errors. Further, the resolution of our modeled depths and velocities and ensuing feeding station spacing (1 m) were greater than the maximum calculated reaction distances and did not allow for fish to move from one feeding station to another (Hafs et al. 2014). Advances in remote sensing techniques are constantly improving accuracy, resolution, and spatial coverage to provide better support for the type of framework we have proposed here (e.g., advent of image analysis, like structure from motion, from unmanned aerial vehicles; Woodget et al. 2015; Dietrich 2016; Tomsett and Leyland 2019).

Understanding the complex feedbacks among habitat degradation, water and land use, restoration activities, and the predictions of such activities on river ecosystem status requires holistic and fine-resolution modeling techniques, which have not been available. To address this knowledge gap, we developed a novel approach to bioenergetics modeling, which leveraged new topobathymetric LiDAR technology, two-dimensional numerical flow modeling, and publicly available fisheries and habitat data. This

new approach allowed for the assessment of morphological impacts and water use on juvenile Chinook salmon habitat suitability. Our modeling demonstrates that removing diversions, and thus returning the flow regime to its natural condition, is not sufficient to revert the impact of anthropogenic activities and may be detrimental in the short period without simultaneously focusing on in-channel morphology. Water diversion reduction towards natural flows needs to be accompanied by increasing lateral connectivity and main channel flow complexity. Anthropogenically simplified, mainstem areas currently have flow velocity too fast to maintain bioenergetic conditions that support growth for a natural flow regime.

Our results highlight the importance of restoration activities that construct and reconnect lateral habitat to the main channel, develop slow water areas, and increase the overall channel length to increase the total suitable area as flow approaches natural conditions. Increase in flow complexity and preserving local low velocities could be achieved with both abiotic and biotic strategies and their combination. The former could include reintroduction of large woody debris, reconnection of side channels, followed by adequate maintenance flows, and the latter with healthy riparian vegetation, which produces natural wood recruitment and reintroduction of native riverine mammals like beavers (*Castor canadensis*). These strategies may provide process-driven channel scour and lateral movement into the flood plain that could help increase overall suitable area. Though not all strategies are adequate for all streams, an approach as that proposed in this study could help identify the most suitable life-stage-specific set of solutions.

This study further demonstrates the utility of remotely sensed topobathymetry and LiDAR-supported numerical flow modeling, meanwhile building upon biological-data-supported bioenergetic modeling to assess water use and channel simplification on aquatic habitat distribution beyond the traditional limited reach scale (10–20 bankfull channel widths or a few hundred metres). These results and methodologies could be adapted and applied to other watersheds to gain more comprehensive understanding and address limiting factors to help ecosystem recovery or guide construction of new ecosystems. Studies such as this allow for development of a virtual stream where processes can be studied at the proper resolution and length scale and alternative strategies can be evaluated. Although returning the natural flow regime (removing diversion in this case) without adequate morphological enhancements may not lead to the expected restoration outcomes in the short term, but could even be detrimental, it may have beneficial effects at a long time scale. At an extended time scale (e.g., decades), stream morphology will readjust to the hydrological and sediment input regime. This suggests that restoration activities should evaluate both short- and long-term effects of re-establishing a near natural flow and whether passive (without morphological restoration), enhancement (small morphological changes in ad hoc location), and active (with morphological adjustment) restorations would be better for the goals and expected outcomes.

References

Allan, J.D. 1978. Trout predation and the size composition of stream drift. Limnol. Oceanogr. **23**(6): 1231–1237. doi:10.4319/lo.1978.23.6.1231.

Arthaud, D.L., Greene, C.M., Guilbault, K., and Morrow, J.V. 2010. Contrasting life-cycle impacts of stream flow on two Chinook salmon populations. Hydrobiologia, **655**(1): 171–188. doi:10.1007/s10750-010-0419-0.

Beechie, T.J., Sear, D.A., Olden, J.D., Pess, G.R., Buffington, J.M., Moir, H., et al. 2010. Process-based principles for restoring river ecosystems. Bioscience, **60**(3): 209–222. doi:10.1525/bio.2010.60.3.7.

Benjankar, R., Tonina, D., and Mckean, J. 2015. One-dimensional and two-dimensional hydrodynamic modeling derived flow properties: impacts on aquatic habitat quality predictions. Earth Surf. Process. Landforms, **40**(3): 340–356. doi:10.1002/esp.3637.

Benjankar, R., Tonina, D., Marzadri, A., McKean, J., and Isaak, D.J. 2016. Effects of habitat quality and ambient hyporheic flows on salmon spawning site selection. J. Geophys. Res. Biogeosci. **121**(5): 1222–1235. doi:10.1002/2015JG003079.

Bennett, S., Pess, G., Bouwes, N., Roni, P., Bilby, R.E., Gallagher, S., et al. 2016. Progress and challenges of testing the effectiveness of stream restoration in the Pacific Northwest using intensively monitored watersheds. Fisheries, **41**(2): 92–103. doi:10.1080/03632415.2015.1127805.

Bernhardt, E.S. 2005. Ecology: synthesizing U.S. river restoration efforts. Science, **308**(5722): 636–637. doi:10.1126/science.1109769. PMID:15860611.

Bisson, P.A., Dunham, J.B., and Reeves, G.H. 2009. Synthesis, part of a special feature on pathways to resilient salmon ecosystems freshwater ecosystems and resilience of Pacific Salmon: habitat management based on natural variability. Ecol. Soc. **14**(1). doi:10.5751/ES-02784-140145.

Bjornn, T.C. 1971. Trout and salmon movements in two Idaho streams as related to temperature, food, stream flow, cover, and population density. Trans. Am. Fish. Soc. **100**(3): 423–438. doi:10.1577/1548-8659(1971)100<423:TASMIT>2.0.CO;2.

Bond, M.H., Nodine, T.G., Beechie, T.J., and Zabel, R.W. 2019. Estimating the benefits of widespread floodplain reconnection for Columbia River Chinook salmon. Can. J. Fish. Aquat. Sci. **76**(7): 1212–1226. doi:10.1139/cjfas-2018-0108.

Brooker, D.J. 2016. Generalized models of riverine fish hydraulic habitat. J. Ecohydraulics, **1**(1–2): 31–49. doi:10.1080/24705357.2016.1229141.

CHaMP. 2014. Scientific protocol for salmonid habitat surveys within the Columbia Habitat Monitoring Program. Prepared by the Integrated Status and Effectiveness Monitoring Program and published by Terraqua, Inc., Wauconda, Wash.

Chapman, D.W. 1962. Aggressive behavior in juvenile coho salmon as a cause of emigration. J. Fish. Res. Board Can. **19**(6): 1047–1080. doi:10.1139/f62-069.

Chittaro, P.M., Zabel, R.W., Haught, K., Sanderson, B.L., and Kennedy, B.P. 2014. Spatial and temporal patterns of growth and consumption by juvenile spring/summer Chinook salmon *Oncorhynchus tshawytscha*. Environ. Biol. Fishes, **97**(12): 1397–1409. doi:10.1007/s10641-014-0230-2.

Cohen, P., Andriamahefa, H., and Wasson, J.-G. 1998. Towards a regionalization of aquatic habitat: distribution of mesohabitats at the scale of a large basin. Regul. Rivers Res. Manage. **14**(1): 391–404. doi:10.1002/(SICI)1099-1646(199809/10)14:5<391::AID-RRR513>3.0.CO;2-W.

Copeland, T., Venditti, D.A., and Barnett, B.R. 2014. The importance of juvenile migration tactics to adult recruitment in stream-type Chinook salmon populations. Trans. Am. Fish. Soc. **143**(6): 1460–1475. doi:10.1080/00028487.2014.949011.

Danish Hydraulic Institute. 2000. MIKE21 flow model, hydrodynamic module, scientific documentation. Denmark.

Davis, J., O'Grady, A.P., Dale, A., Arthington, A.H., Gell, P.A., Driver, P.D., et al. 2015. When trends intersect: the challenge of protecting freshwater ecosystems under multiple land use and hydrological intensification scenarios. Sci. Total Environ. **534**: 65–78. doi:10.1016/j.scitotenv.2015.03.127.

Deslauriers, D., Resource, N., and Dakota, S. 2017. Fish bioenergetics 4.0: an R-based modeling application. Fisheries, **42**(11): 586–596. doi:10.1080/03632415.2017.1377558.

Dietrich, J.T. 2016. Riverscape mapping with helicopter-based Structure-from-Motion photogrammetry. Geomorphology, **252**: 144–157. doi:10.1016/j.geomorph.2015.05.008.

Dodrill, M.J., Yackulic, C.B., Kennedy, T.A., and Hayes, J.W. 2016. Prey size and availability limits maximum size of rainbow trout in a large tailwater: insights from a drift-foraging bioenergetics model. Can. J. Fish. Aquat. Sci. **73**(5): 759–772. doi:10.1139/cjfas-2015-0268.

Elliott, J.M. 1975. Number of meals in a day, maximum weight of food consumed in a day and maximum rate of feeding for brown trout, *Salmo trutta* L. Freshw. Biol. **5**(3): 287–303. doi:10.1111/j.1365-2427.1975.tb00142.x.

Elliott, J.M. 1976. The energetics of feeding, metabolism and growth of brown trout (*Salmo trutta* L.) in relation to body weight, water temperature and ration size. J. Anim. Ecol. **45**(3): 923–948. doi:10.2307/3590.

Esri. 2017. ArcGIS release 10.6. Redlands, Calif.

Fausch, K.D. 2014. A historical perspective on drift foraging models for stream salmonids. Environ. Biol. Fishes, **97**(5): 453–464. doi:10.1007/s10641-013-0187-6.

Goodwin, R.A., Nestler, J.M., Anderson, J.J., Weber, L.J., and Loucks, D.P. 2006. Forecasting 3-D fish movement behavior using a Eulerian–Lagrangian-agent method (ELAM). Ecol. Modell. **192**(1–2): 197–223. doi:10.1016/j.ecolmodel.2005.08.004.

Guensch, G.R., Hardy, T.B., and Addley, R.C. 2001. Examining feeding strategies and position choice of drift-feeding salmonids using an individual-based, mechanistic foraging model. Can. J. Fish. Aquat. Sci. **58**(3): 446–457. doi:10.1139/f00-257.

Gustafson, R.G., Waples, R.S., Myers, J.M., Weitkamp, L.A., Bryant, G.J., Johnson, O.W., and Hard, J.J. 2007. Pacific salmon extinctions: quantifying lost and remaining diversity. Conserv. Biol. **21**(4): 1009–1020. doi:10.1111/j.1523-1739.2007.00693.x. PMID:17650251.

Hafs, A.W., Harrison, L.R., Utz, R.M., and Dunne, T. 2014. Quantifying the role of woody debris in providing bioenergetically favorable habitat for juvenile salmon. Ecol. Modell. **285**: 30–38. doi:10.1016/j.ecolmodel.2014.04.015.

Hayes, J.W., Hughes, N.F., and Kelly, L.H. 2007. Process-based modelling of invertebrate drift transport, net energy intake and reach carrying capacity for drift-feeding salmonids. Ecol. Modell. **207**(2–4): 171–188. doi:10.1016/j.ecolmodel.2007.04.032.

Healey, M.C. 1992. Life history of Chinook salmon (*Oncorhynchus tshawytscha*). *In* Pacific salmon life histories. doi:10.2307/1446178.

Hering, D., Borja, A., Carstensen, J., Carvalho, L., Elliott, M., Feld, C.K., et al. 2010.

The European Water Framework Directive at the age of 10: a critical review of the achievements with recommendations for the future. Sci. Total Environ. **408**(19): 4007–4019. doi:10.1016/j.scitotenv.2010.05.031. PMID:20557924.

Hughes, N.F., and Dill, L.M. 1990. Position choice by drift-feeding Salmonids: model and test for Arctic Grayling (*Thymallus arcticus*) in subarctic mountain streams, interior Alaska. Can. J. Fish. Aquat. Sci. **47**(10): 2039–2048. doi:10.1139/f90-228.

Isaak, D.J., and Thurow, R.F. 2006. Network-scale spatial and temporal variation in Chinook salmon (*Oncorhynchus tshawytscha*) redd distributions: patterns inferred from spatially continuous replicate surveys. Can. J. Fish. Aquat. Sci. **63**(2): 285–296. doi:10.1139/f05-214.

Isaak, D.J., Wenger, S.J., Peterson, E.E., Ver Hoef, J.M., Nagel, D.E., Luce, C.H., et al. 2017. The NorWeST summer stream temperature model and scenarios for the western U.S.: a crowd-sourced database and new geospatial tools foster a user community and predict broad climate warming of rivers and streams. Water Resour. Res. **53**(11): 9181–9205. doi:10.1002/2017WR020969.

Jenkins, A.R., and Keeley, E.R. 2010. Bioenergetic assessment of habitat quality for stream-dwelling cutthroat trout (*Oncorhynchus clarkii bouvieri*) with implications for climate change and nutrient supplementation. Can. J. Fish. Aquat. Sci. **67**(2): 371–385. doi:10.1139/F09-193.

Jorde, K., Schneider, M., Peter, A., and Zoellner, F. 2001. Fuzzy based models for the evaluation of fish habitat quality and instream flow assessment. *In* Proceedings of the 3rd International Symposium on Environmental Hydraulics, 5–8 December, Tempe, Ariz. (January). pp. 1–6.

Kalleberg, H. 1958. Observations in a stream tank of territoriality and competition in juvenile salmon and trout. Rep. Inst. Freshw. Res. Drottningholm, **39**: 55–98. Available from http://ci.nii.ac.jp/naid/10006681223/en/ [accessed 6 November 2019].

Kammel, L.E., Pasternack, G.B., Massa, D.A., and Bratovich, P.M. 2016. Near-census ecohydraulics bioverification of *Oncorhynchus mykiss* spawning microhabitat preferences. J. Ecohydraulics, **1**(1–2): 62–78. doi:10.1080/24705357.2016.1237264.

Keeley, E.R., Campbell, S.O., and Kohler, A.E. 2016. Bioenergetic calculations evaluate changes to habitat quality for salmonid fishes in streams treated with salmon carcass analog. Can. J. Fish. Aquat. Sci. **73**(5): 819–831. doi:10.1139/cjfas-2015-0265.

Legleiter, C.J., Kyriakidis, P.C., McDonald, R.R., and Nelson, J.M. 2011. Effects of uncertain topographic input data on two-dimensional flow modeling in a gravel-bed river. Water Resour. Res. **47**(3): 1–24. doi:10.1029/2010WR009618.

Leung, E.S., Rosenfeld, J.S., and Bernhardt, J.R. 2009. Habitat effects on invertebrate drift in a small trout stream: implications for prey availability to drift-feeding fish. Hydrobiologia, **623**(1): 113–125. doi:10.1007/s10750-008-9652-1.

Maret, T.R., Hortness, J.E., and Ott, D.S. 2005. Instream flow characterization of Upper Salmon River Basin streams, Central Idaho, 2005.

Mason, J.C., and Chapman, D.W. 1965. Significance of early emergence, environmental rearing capacity, and behavioral ecology of juvenile Coho salmon in stream channels. J. Fish. Res. Board Can. **22**(1): 173–190. doi:10.1139/f65-015.

McKean, J., and Tonina, D. 2013. Bed stability in unconfined gravel bed mountain streams: with implications for salmon spawning viability in future climates. J. Geophys. Res. Earth Surf. **118**(3): 1227–1240. doi:10.1002/jgrf.20092.

McKean, J.A., Isaak, D.J., and Wright, C.W. 2008. Geomorphic controls on salmon nesting patterns described by a new, narrow-beam terrestrial–aquatic lidar. Front. Ecol. Environ. **6**(3): 125–130. doi:10.1890/070109.

McKean, J., Tonina, D., Bohn, C., and Wright, C.W. 2014. Effects of bathymetric lidar errors on flow properties predicted with a multi-dimensional hydraulic model. J. Geophys. Res. Earth Surf. **119**(3): 644–664. doi:10.1002/2013JF002897.

Morton, C., Knowler, D., Brugere, C., Lymer, D., and Bartley, D. 2017. Valuation of fish production services in river basins: a case study of the Columbia River. Ecosyst. Serv. **24**: 101–113. doi:10.1016/j.ecoser.2017.02.007.

Naman, S.M., Rosenfeld, J.S., Third, L.C., and Richardson, J.S. 2017. Habitat-specific production of aquatic and terrestrial invertebrate drift in small forest streams: implications for drift-feeding fish. Can. J. Fish. Aquat. Sci. **74**(8): 1208–1217. doi:10.1139/cjfas-2016-0406.

Newman, M.A. 1956. Social behavior and interspecific competition in two trout species. Physiol. Zool. **29**(1): 64–81. doi:10.1086/physzool.29.1.30152381.

Newson, M.D., and Newson, C.L. 2000. Geomorphology, ecology and river channel habitat: mesoscale approaches to basin-scale challenges. Prog. Phys. Geogr. **24**(2): 195–217. doi:10.1177/030913330002400203.

NMFS. 2014. NOAA's National Marine Fisheries Service, Northwest Region, Endangered Species Act Section 7(a)(2) Supplemental Biological Opinion. Consultation on remand for operation of the federal Columbia River Power System. NOAA Fisheries Log Number: NWR-2013-9562.

NOAA. 2008. Supplemental comprehensive analysis of the Federal Columbia River Power System and mainstem effects of the Upper Snake and other tributary actions.

NOAA. 2011. Five-year review: summary & evaluation of middle Columbia River steelhead.

Noack, M., Schneider, M., and Wieprecht, S. 2013. The habitat modelling system CASiMiR: a multivariate fuzzy approach and its applications. *In* Ecohydraulics: an integrated approach. pp. 75–91. doi:10.1002/9781118526576.ch4.

Palmer, M.A., Menninger, H.L., and Bernhardt, E. 2010. River restoration, habitat heterogeneity and biodiversity: a failure of theory or practice? Freshw. Biol. **55**(Suppl. 1): 205–222. doi:10.1111/j.1365-2427.2009.02372.x.

Railsback, S.F., Gard, M., Harvey, B.C., White, J.L., and Zimmerman, J.K.H. 2013. Contrast of Degraded and restored stream habitat using an individual-based salmon model. N. Am. J. Fish. Manage. **33**(2): 384–399. doi:10.1080/02755947.2013.765527.

Rand, P.S., Goslin, M., Gross, M.R., Irvine, J.R., Augerot, X., McHugh, P.A., and Bugaev, V.F. 2012. Global assessment of extinction risk to populations of Sockeye salmon *Oncorhynchus nerka*. PLoS ONE, **7**(4). doi:10.1371/journal.pone.0034065. PMID:22511930.

Roni, P., Anders, P.J., Beechie, T.J., and Kaplowe, D.J. 2018. Review of tools for identifying, planning, and implementing habitat restoration for pacific salmon and steelhead. J. Fish. Manage. **38**: 355–376. doi:10.1002/nafm.10035.

Rosenfeld, J.S., and Boss, S. 2011. Fitness consequences of habitat use for juvenile cutthroat trout: energetic costs and benefits in pools and riffles. Can. J. Fish. Aquat. Sci. **58**(3): 585–593. doi:10.1139/f01-019.

Rosenfeld, J.S., and Taylor, J. 2009. Prey abundance, channel structure and the allometry of growth rate potential for juvenile trout. Fish. Manage. Ecol. **16**(3): 202–218. doi:10.1111/j.1365-2400.2009.00656.x.

Rosenfeld, J.S., Bouwes, N., Wall, C.E., and Naman, S.M. 2014. Successes, failures, and opportunities in the practical application of drift-foraging models. Environ. Biol. Fishes, **97**(5): 551–574. doi:10.1007/s10641-013-0195-6.

Schwartz, J.S. 2016. Use of ecohydraulic-based mesohabitat classification and fish species traits for stream restoration design. Water, **8**(11): 1–33. doi:10.3390/w8110520.

Tomsett, C., and Leyland, J. 2019. Remote sensing of river corridors: a review of current trends and future directions. River Res. Appl. **35**: 779–803. doi:10.1002/rra.3479.

Tonina, D., McKean, J.A., Benjankar, R.M., Wright, W., Goode, J.R., Chen, Q., et al. 2018. Mapping river bathymetries: evaluating topobathymetric LiDAR survey. Earth Surf. Process. Landforms, **44**: 507–520. doi:10.1002/esp.4513.

Wall, C.E., Bouwes, N., Wheaton, J.M., Saunders, W.C., and Bennett, S.N. 2016. Net rate of energy intake predicts reach-level steelhead (*Oncorhynchus mykiss*) densities in diverse basins from a large monitoring program. Can. J. Fish. Aquat. Sci. **73**(7): 1081–1091. doi:10.1139/cjfas-2015-0290.

Walters, A.W., Bartz, K.K., and Mcclure, M.M. 2013. Interactive Effects of Water Diversion and Climate Change for Juvenile Chinook Salmon in the Lemhi River Basin (USA.). Conserv. Biol. **27**(6): 1179–1189. doi:10.1111/cobi.12170. PMID:24299084.

Weber, N., Bouwes, N., Jordan, C.E., and Jonsson, B. 2014. Estimation of salmonid habitat growth potential through measurements of invertebrate food abundance and temperature. Can. J. Fish. Aquat. Sci. **71**(8): 1158–1170. doi:10.1139/cjfas-2013-0390.

Wheaton, J.M., Bouwes, N., Mchugh, P., Saunders, C., Bangen, S., Bailey, P., et al. 2018. Upscaling site-scale ecohydraulic models to inform salmonid population-level life cycle modeling and restoration actions — lessons from the Columbia River Basin. Earth Surf. Process. Landforms, **43**(1): 21–44. doi:10.1002/esp.4137.

Wilzbach, M.A., and Hall, J.D. 1985. Prey availability and foraging behavior of cutthroat trout in an open and forested section of stream. SIL Proc. 1922–2010, **22**(4): 2516–2522. doi:10.1080/03680770.1983.11897715.

Wohl, E., Lane, S.N., and Wilcox, A.C. 2015. The science and practice of river restoration. Water Resour. Res. **51**(8): 5974–5997. doi:10.1002/2014WR016874.

Woodget, A.S., Carbonneau, P.E., Visser, F., and Maddock, I.P. 2015. Quantifying submerged fluvial topography using hyperspatial resolution UAS imagery and structure from motion photogrammetry. Earth Surf. Process. Landforms, **40**(1): 47–64. doi:10.1002/esp.3613.

Woodward, G., Perkins, D.M., and Brown, L.E. 2010. Climate change and freshwater ecosystems: impacts across multiple levels of organization. Philos. Trans. R. Soc. B Biol. Sci. **365**(1549): 2093–2106. doi:10.1098/rstb.2010.0055. PMID:20513717.